

Effect of Depolarizing and Quenching Collisions on the Contrast of Coherent Population Trapping Resonance

K.M. Sabakar,¹ M.I. Vaskovskaya¹,[✉] D.S. Chuchelov,¹ E.A. Tsygankov^{1,*},[✉] V.V. Vassiliev¹,[✉] S.A. Zibrov,¹ and V.L. Velichansky^{1,2}

¹Lebedev Physical Institute of the Russian Academy of Sciences, Leninsky Prospect 53, Moscow 119991, Russia

²National Research Nuclear University MEPhI, Kashirskoye Highway 31, Moscow 115409, Russia

(Received 3 May 2023; revised 26 July 2023; accepted 16 August 2023; published 8 September 2023)

We investigate the effect of buffer gases on the coherent population trapping resonance induced by a σ -polarized optical field in ^{87}Rb atoms. Our experimental results show that inert gases, which depolarize the excited state of alkali-metal atoms, provide higher contrast than nitrogen that effectively quenches their fluorescence. We also demonstrate that elimination of spontaneous radiation does not significantly decrease the width at moderate temperatures of an atomic medium. Therefore, a mixture of inert gases can be preferable over a mixture with nitrogen for atomic clocks.

DOI: 10.1103/PhysRevApplied.20.034015

I. INTRODUCTION

All-optical interrogation schemes utilizing the effect of coherent population trapping (CPT) [1], progress in miniature vapor-cell production technology, and advances in diode lasers [2] have led to the development of chip-scale atomic clocks [3]. Their main advantages over other frequency standards are smaller size and lower power consumption, but they also have lower frequency stability. Currently, many research groups are seeking new approaches to improve the long-term frequency stability of such atomic clocks [4–7]. In the absence of a frequency drift, the stability is proportional to $1/\sqrt{\tau}$, where τ is the averaging time [8]. In this case, a further improvement of the long-term frequency stability can be achieved only by the increase of the short-term stability, which depends on the contrast-to-width ratio of the CPT resonance. In what follows, we call this the quality factor or Q -factor.

The standard approach to reduce the relaxation rate of the ground-state coherence occurring due to collisions of alkali-metal atoms with atomic cell walls is the usage of a buffer gas. This provides diffusion of atoms to the walls with a slower speed than their unperturbed movement with the thermal velocity. The probability of losing the polarization upon collisions with buffer gas particles is less than under interaction with the cell walls. However, an increase in the buffer gas pressure eventually results in the collisional rebroadening of the CPT resonance. These opposite dependencies give the value of buffer gas pressure that provides the minimum width. This value depends on the dimensions and geometry of the cell [9]. The buffer

gas induces a temperature-dependent shift of the CPT resonance frequency, which can be suppressed by using a mixture of two gases with linear temperature coefficients of opposite signs [10]. Most often, a mixture of argon and nitrogen is used.

It is known that inert gases depolarize the excited state of alkali-metal atoms and tend to equalize populations of its magnetic sublevels [11–14]. The equalization of populations should increase the CPT resonance amplitude detected in the $\sigma^+ - \sigma^+$ scheme. Indeed, the depolarization reduces the number of atoms pumped to the sublevel $5\text{P}_{1/2}$ $m_{F_e} = 2$ (we consider the case of ^{87}Rb atoms). Therefore, a smaller amount of atoms is optically pumped to the nonabsorbing sublevel $m_{F_g} = 2$ of the ground state and more atoms arrive at the working sublevels $F_g = 1, 2$, $m_{F_g} = 0$ due to spontaneous transitions. Figure 1 demonstrates the distribution of populations over magnetic sublevels for the cases of zero and complete excited-state depolarization. These were obtained by solving density-matrix equations accounting for all electric-dipole transitions of the D_1 line induced by a bichromatic σ^+ -polarized optical field. The power broadening of the CPT resonance was set to be three times greater than the relaxation rate of ground-state elements to make difference in populations evident. Details of calculations are given in the Appendix.

Nitrogen quenches fluorescence of alkali-metal atoms due to the transfer of the excited-state energy to molecular vibrations. This prevents broadening of the CPT resonance induced by the spontaneous radiation, therefore nitrogen is often considered a preferable buffer gas for atomic clocks [9,15]. Transitions from the excited to the ground states during quenching have the same selection rules as spontaneous decay [16,17], but the effect of nitrogen on the

*tsygankov.e.a@yandex.ru

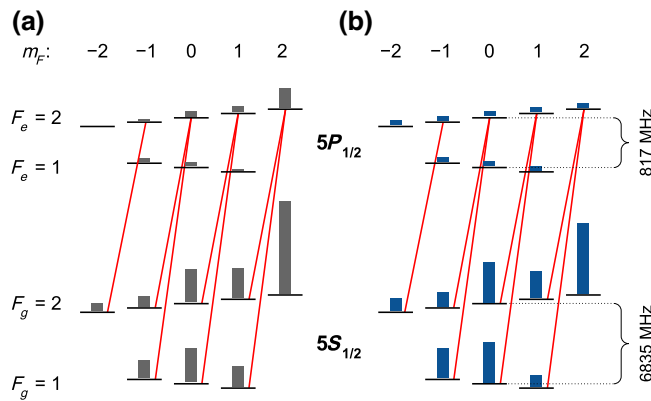


FIG. 1. Energy-level structure and electric-dipole transitions to sublevels of hyperfine component $F_e = 2$ induced by an optical field with σ^+ polarization. Columns show the distribution of populations over $5S_{1/2}$ and $5P_{1/2}$ states. These were calculated in a model (a) without and (b) with accounting for the depolarization; see the Appendix for details. The heights of the columns for the excited state are increased by about five orders of magnitude.

population distribution of the excited state has not been studied in detail and is poorly described in the literature.

We assume that quenching and depolarization are competitive processes since their probabilities are comparable [9,14], that is, there are collisions where a nonradiative transition occurs without mixing of upper-state sublevels. Therefore, quenching molecular gases should provide a smaller equalization of the excited-state populations than inert ones. In this case, nitrogen should reduce the CPT resonance amplitude compared to inert gases while improving its width due to the elimination of the spontaneous radiation. These two factors have opposing influence on the Q -factor. The goal of this paper is to estimate which of them is more significant. To check this, we compared the contrast and width of the CPT resonance in Ar, Ne, and N₂.

II. EXPERIMENT

The experimental setup is schematically shown in Fig. 2. We used a single-mode vertical-cavity surface-emitting laser (VCSEL) generating at approximately 795 nm. The dc and rf components of the injection current were fed to the laser via a bias tee. The modulation frequency was close to 3.417 GHz, and the first sidebands of the polychromatic optical field were tuned to transitions $F_g = 2 \rightarrow F_e = 2$, $F_g = 1 \rightarrow F_e = 2$ of the $^{87}\text{Rb D}_1$ line. When the frequency difference of the first sidebands coincides with that of the transition between sublevels $m_{F_g} = 0$ of the ground state, a nonabsorbing superposition arises which increases transmission of the optical field. The power of the rf field was set to provide the highest amplitudes of the first-order sidebands. A polarizer and a quarter-wave plate were used to form the CPT resonance in the $\sigma^+ - \sigma^+$ scheme. The diameter of the laser beam was 3 mm. The

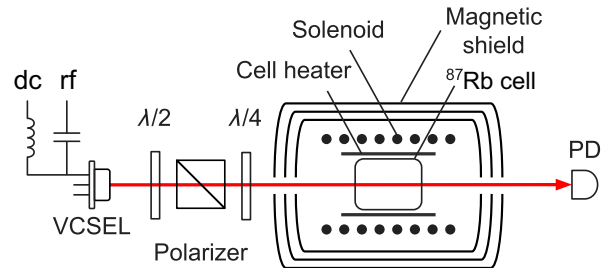


FIG. 2. The layout of the experimental setup.

laser wavelength was stabilized by a feedback loop that controls the temperature of the laser diode.

An atomic cell was placed in a longitudinal magnetic field of 0.02 G to separate the metrological CPT resonance from magnetosensitive ones at the transitions between sublevels $m_{F_g} = \pm 1$. The temperature of the atomic cell was maintained to an accuracy of 0.01 °C. The cell, heater, and solenoid were placed in a three-layer μ -metal magnetic shield, providing better than 500-fold suppression of the laboratory magnetic field.

We manufactured three sets of cylindrical atomic cells with CO₂ laser-welded windows (8 mm diameter, 15 mm length, 0.7 mm wall thickness) and filled them with isotopically enriched ^{87}Rb and a buffer gas: N₂, Ar, or Ne. The buffer gas pressures were 30, 60, and 90 torr. We used pinch-off glass welding to seal the stem at a distance of about 20 mm from the cell body so as not to heat it. This ensured that the actual gas pressure inside the cell differed from the pressure in the filling chamber by no more than 1%.

Figure 3 shows metrological and magnetosensitive CPT resonances obtained in two atomic cells filled with nitrogen and argon at a pressure of 90 torr. The inhomogeneity of the magnetic field did not lead to a noticeable broadening of magnetosensitive resonances, thus we consider their amplitudes to be determined by populations of the corresponding magnetic sublevels. Experimental conditions were the same for both cells: the temperature was 65 °C and the optical field intensity was 0.3 mW/cm². The nonresonant radiation losses in both cells were almost equal. However, some differences in the signals can be seen. First, resonances on sublevels $F_g = 1, 2, m_{F_g} = -1$ (left) and $F_g = 1, 2, m_{F_g} = 0$ (central) have noticeably greater amplitudes in Ar than in N₂. Second, the background transmission in nitrogen is higher when the microwave frequency is detuned from the CPT resonance (approximately 1.96 V in N₂, approximately 1.82 V in Ar). On the contrary, nitrogen should provide a slightly smaller transmission level due to the lower collisional broadening of the $^{87}\text{Rb D}_1$ line [18]. We attribute the features mentioned above to the negative impact of the fluorescence quenching in nitrogen, which reduces efficiency of the excited state

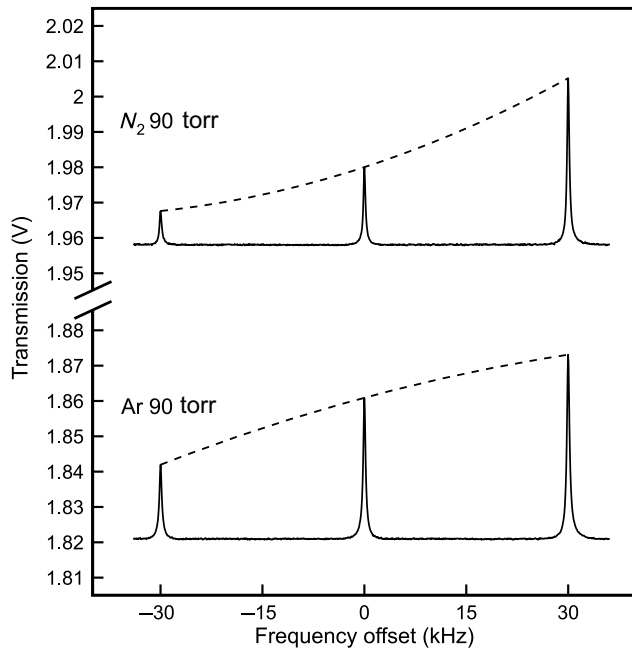


FIG. 3. Metrological (central) and magnetosensitive CPT resonances obtained in atomic cells filled with nitrogen and argon at a pressure of 90 torr. The dashed lines serve as a guide for the eye and show the difference in the amplitudes of the resonances.

depolarization and enhances pumping to the nonabsorbing sublevel.

Dependencies of the contrast (the ratio of the resonance amplitude to the transmission level at resonance peak) of the metrological CPT resonance on the laser field intensity for all pressures are shown in Fig. 4. The difference in contrast between gases is negligible at intensities below 0.1 mW/cm^2 for all pressures. As the intensity increases, the rate of optical pumping becomes significant and a divergence between dependencies arises. For N_2 , the contrast reaches a maximum and then slightly decreases. For Ar and Ne the contrast does not decrease even at the highest available intensity of 1 mW/cm^2 . Neon provides

the highest contrast, reaching a value of 6.5%, while the maximal contrasts for argon and nitrogen are 5% and 3.6%, respectively. As the pressure increases, the dependencies remain almost the same and the relation $C_{\max}^{\text{Ne}} > C_{\max}^{\text{Ar}} > C_{\max}^{\text{N}_2}$ does not change, but the maximal contrasts decline. Thus happens due to the growth of homogeneous broadening that leads to decrease in amount of atoms optically pumped into the dark state. The increase in temperature cannot fully compensate the loss in number of atoms since the relaxation rate of the ground-state coherence becomes greater due to the spin-exchange mechanism. Therefore, the maximal absorption contrast is achieved at higher temperature for greater buffer gas pressure and falls with growth of the latter. The difference in contrasts between the inert gases is due to the smaller broadening of $^{87}\text{Rb D}_1$ line by Ne [18].

Similarly to the contrast, the dependencies of the CPT resonance width and Q -factor on the intensity were obtained. From each dependence $Q(I)$ we defined the maximum value Q_{\max} and plotted the dependence of the Q_{\max} on temperature for each gas and all pressures (Fig. 5). Under the same conditions, the resonance in nitrogen has the smallest width. Nitrogen has an advantage over argon and neon of about 20% and 10% in Q_{\max} for a pressure of 30 torr, which is achieved due to the narrower resonance. At higher buffer gas pressures, the advantage of inert gases in contrast exceeds the advantage of nitrogen in width. As a result, $Q_{\max}^{\text{Ne}}/Q_{\max}^{\text{N}_2}$ is close to 1.6 at 60 torr and to 2 at 90 torr. Note that neon maximizes the Q -factor at lower temperatures than other gases at all pressures.

Figures 6(a) and 6(b) shows dependencies of the CPT resonance width on the optical field intensity for different temperatures in neon and nitrogen. In neon the width decreases with temperature at intensities above 0.4 mW/cm^2 . This feature is due to the light narrowing effect [19], which takes place when a sufficiently large number of atoms are coherently trapped in a dark state. In nitrogen, as the temperature increases, the width increases

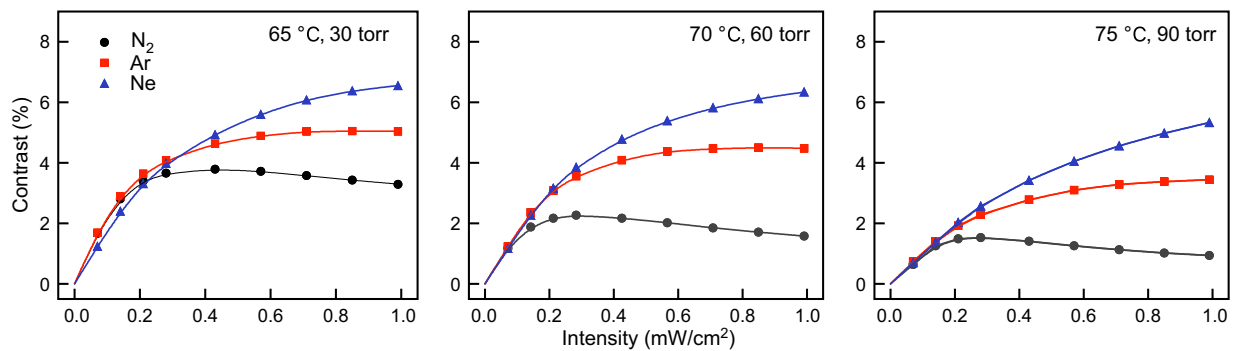


FIG. 4. Dependencies of the CPT resonance contrast on the laser intensity for different temperatures and pressures of nitrogen, argon, and neon.

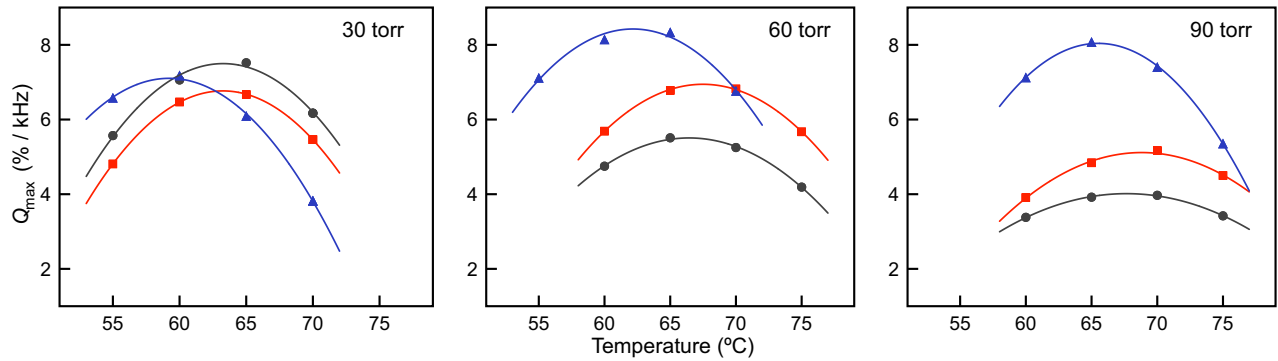


FIG. 5. Dependencies of the maximal (in terms of intensity) quality factor Q_{\max} of the CPT resonance on the cell temperature for different pressures of nitrogen, argon, and neon. The legend is the same as in Fig. 4.

in the same way for all intensities, which indicates the much smaller impact of this effect. Therefore, more atoms reside at the nonabsorbing sublevel in N_2 compared to Ne.

We have studied the potential benefit of fluorescence quenching in nitrogen for the CPT resonance width. For this, we made three additional cells with the same diameter of 8 mm but smaller internal length of 2.5 mm. The decrease in length prevents complete absorption of low-intensity laser radiation at high temperatures and Rb concentrations, when the influence of spontaneous photons on the width should be more evident. The cells were filled with 90 torr of Ar, Ne, and N_2 . The beam was expanded to 6 mm in diameter and the operating radiation intensity was 0.1 mW/cm^2 . The measured dependencies of the CPT resonance width on temperature in these cells are shown in Fig. 6(c). As one would expect, the width should grow faster with temperature in inert gases than in nitrogen due to the spontaneous radiation. However, dependencies in all gases reveal the same behavior, which is typical of

spin-exchange broadening. The contribution of this mechanism to the coherence relaxation is given by [14]

$$\Gamma_{\text{SE}} = \frac{6I + 1}{8I + 4} \sigma_{\text{SE}} v_r n, \quad (1)$$

where I is the nuclear spin, σ_{SE} is the spin-exchange cross-section, v_r is the average relative velocity, and n is the concentration of the alkali-metal atoms. The dashed line in Fig. 6(c) is the dependence of Γ_{SE}/π on temperature for ^{87}Rb plotted for concentration taken from [20] and the most reliable value of σ_{SE} equal to $1.9 \times 10^{-14} \text{ cm}^2$ [21]. However, we have not observed a noticeable broadening of the CPT resonance in inert gases at high temperatures compared to nitrogen. A similar result was obtained earlier in [22] for ^{133}Cs in the temperature range $20\text{--}65^\circ\text{C}$. Thus, we do not associate the difference in widths with the quenching effect; it is probably related to the lower diffusion coefficient in nitrogen [23,24], which determines the rate of Rb coherence relaxation as a result of collisions with the cell walls.

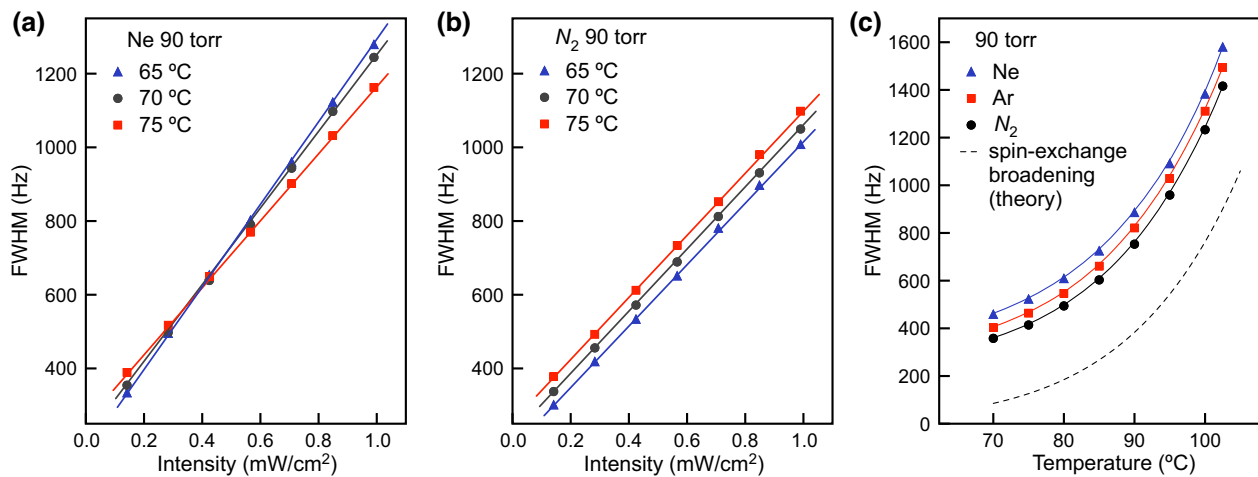


FIG. 6. Dependencies of the CPT resonance width on the optical field intensity for different temperatures in (a) neon and (b) nitrogen and (c) on the temperature for atomic cells with nitrogen, argon and neon. Pressure of all buffer gases is 90 torr. The dashed line in (c) is the spin-exchange broadening for ^{87}Rb calculated via Eq. (1).

III. DISCUSSION

Considering the choice of a buffer gas for CPT-based atomic clocks, we believe that a proper mixture of Ar and Ne is preferable to a mixture containing N₂. When using inert gases, it is possible to achieve a higher resonance contrast due to depolarization of ⁸⁷Rb excited state. Moreover, the maximal *Q*-factor of the resonance in neon is achieved at a lower temperature than in nitrogen, which reduces the clock's power consumption.

Another advantage of an Ar-Ne mixture is the ability to suppress the light shift at higher buffer gas pressures. As we demonstrated in [25], the ac Stark shift of the CPT resonance frequency cannot be eliminated if the homogeneous broadening of optical lines exceeds a certain value. Since the ⁸⁷Rb D₁ line collisional broadening rate for Ne is about 1.5 times smaller than that for N₂ [18], it is possible to obtain the minimal relaxation rate of the coherence and retain the ability to suppress the light shift in miniature atomic cells, which is significant for chip-scale atomic clocks.

Finally, the depolarization of the ⁸⁷Rb excited state in inert gases leads to a smaller difference in populations of the ground-state working sublevels due to the repopulation pumping mechanism. Unequal populations are the source of the CPT resonance asymmetry and the nonlinear dependence of its frequency on the laser field intensity [26]. This hinders the light shift suppression methods based on the laser field intensity modulation (see, for example, [27]).

IV. SUMMARY

We have demonstrated that argon and neon provide a higher contrast of the CPT resonance than nitrogen in the $\sigma^+ - \sigma^+$ scheme. The difference in contrast is significant when the optical pumping rate dominates the ground-state relaxation. We explain this effect as follows. Quenching of alkali-metal atom fluorescence reduces the degree of the excited-state depolarization, which increases the population of the nonabsorbing sublevel. As a result, the amount of atoms that can be optically pumped to the dark state becomes smaller and the amplitude of CPT resonance decreases. We have not found a benefit from quenching of the fluorescence for the width of the CPT resonance at temperatures providing the maximal *Q*-factor. The difference in *Q*-factor between Ne and N₂ increases with the buffer gas pressure, reaching a factor of 2 at 90 torr. Hence, a mixture of inert gases can be more advantageous for CPT-based atomic clocks than a mixture with nitrogen.

ACKNOWLEDGMENTS

The authors receive funding from Russian Science Foundation (Grant No. 19-12-00417).

APPENDIX

Here we consider the following model of optical pumping in a four-level system with moments $F = 2, 1$ in excited and ground states; see Fig. 1. Components of bichromatic optical field,

$$\mathbf{E}(t) = \mathbf{e} \frac{\mathcal{E}}{2} (e^{-i\omega_r t} + e^{-i\omega_b t} + c.c.),$$

where $\mathbf{e} = (\mathbf{e}_x + i\mathbf{e}_y)/\sqrt{2}$, induce transitions between levels $F_g = 2, F_e = 2$ and $F_g = 1, F_e = 2$, respectively, having optical detuning Δ . The corresponding detuning from the $F_e = 1$ level is $\Delta + \omega_e$, where ω_e is the hyperfine splitting of the excited state. Frequency spacing between components is close to hyperfine splitting of the ground state, $\omega_b - \omega_r = \omega_g + \delta$, where detuning δ is much smaller than ω_g . The phenomenological relaxation constant Γ was introduced in equations for optical coherences to account for homogeneous broadening of absorption line occurring under collision of alkali-metal atoms with particles of a buffer gas. We assume that $\gamma \ll \Gamma$, where γ denotes the natural width of the excited state. The Rabi frequency $V = d\mathcal{E}/2\hbar$ contains the reduced dipole matrix element. For simplicity, one phenomenological constant Γ_g is used to describe relaxation of the ground-state sublevels. Finally, we do not account for magnetosensitive CPT resonances and consider only the one between sublevels $m_{F_g} = 0$. Initial equations for elements of the density matrix were obtained via the quantum Liouville equation. They were then simplified by means of the resonant approximation for the optical field (also known as the rotating-wave approximation) and the assumption of the low-saturation regime. The latter means that populations of the excited state are neglected compared to the ground-state ones. Under the resonant approximation, we separate the optical coherences into slowly varying amplitudes and fast oscillating terms, namely, $\rho_{ij}^{u2} \rightarrow \tilde{\rho}_{ij}^{u2} e^{-i\omega_r t}$, $\rho_{ij}^{d2} \rightarrow \tilde{\rho}_{ij}^{d2} e^{-i\omega_r t}$ for electric-dipole transitions from $F_g = 2$ to the excited state and $\rho_{ij}^{u1} \rightarrow \tilde{\rho}_{ij}^{u1} e^{-i\omega_b t}$, $\rho_{ij}^{d1} \rightarrow \tilde{\rho}_{ij}^{d1} e^{-i\omega_b t}$ for $F_g = 1$, respectively. Here superscripts u and d on the density matrix elements denote upper-state levels $F_e = 2, 1$, and 2 and 1 denote ground-state levels $F_g = 2, 1$. Subscripts denote m_F values. The optical field considered has right circular polarization; therefore, $i = j + 1$. Since components of the optical field induce oscillations of the ground-state coherence at the frequency $\omega_b - \omega_r$, we also introduce slowly varying amplitude and fast oscillating terms in a similar manner: $\rho_{00}^{21} \rightarrow \tilde{\rho}_{00}^{21} e^{-i(\omega_b - \omega_r)t}$. The upper symbol \sim is omitted further for brevity. Under these steps, the excited state can be adiabatically eliminated; by neglecting the terms oscillating at doubled frequencies ω_r, ω_b and omitting the time derivatives of its populations and coherences, we can express them via elements of the ground state. The system of equations for the excited-state populations is as

follows:

$$\rho_{-2-2}^{uu} = 0, \quad (\text{A1a})$$

$$\rho_{-1-1}^{uu} = \frac{V^2}{6} \frac{\Gamma/(\gamma/2)}{\Delta^2 + \Gamma^2} \rho_{-2-2}^{22}, \quad (\text{A1b})$$

$$\rho_{-1-1}^{dd} = \frac{V^2}{2} \frac{\Gamma/(\gamma/2)}{(\Delta + \omega_e)^2 + \Gamma^2} \rho_{-2-2}^{22}, \quad (\text{A1c})$$

$$\rho_{00}^{uu} = \frac{V^2}{4} \frac{\Gamma/(\gamma/2)}{\Delta^2 + \Gamma^2} \left(\rho_{-1-1}^{22} + \frac{1}{3} \rho_{-1-1}^{11} \right), \quad (\text{A1d})$$

$$\rho_{00}^{dd} = \frac{V^2}{4} \frac{\Gamma/(\gamma/2)}{(\Delta + \omega_e)^2 + \Gamma^2} \left(\rho_{-1-1}^{22} + \frac{1}{3} \rho_{-1-1}^{11} \right), \quad (\text{A1e})$$

$$\rho_{11}^{uu} = \frac{V^2}{4} \frac{\Gamma/(\gamma/2)}{\Delta^2 + \Gamma^2} [\rho_{00}^{22} + \rho_{00}^{11} - 2\text{Re}(\rho_{00}^{21})], \quad (\text{A1f})$$

$$\rho_{11}^{dd} = \frac{V^2}{12} \frac{\Gamma/(\gamma/2)}{(\Delta + \omega_e)^2 + \Gamma^2} [\rho_{00}^{22} + \rho_{00}^{11} - 2\text{Re}(\rho_{00}^{21})], \quad (\text{A1g})$$

$$\rho_{22}^{uu} = \frac{V^2}{2} \frac{\Gamma/(\gamma/2)}{\Delta^2 + \Gamma^2} \left(\frac{1}{3} \rho_{11}^{22} + \rho_{11}^{11} \right). \quad (\text{A1h})$$

Populations ρ_{11}^{uu} , ρ_{11}^{dd} are determined not only by optical coherences $\tilde{\rho}_{10}^{u2}$, $\tilde{\rho}_{10}^{u1}$ and $\tilde{\rho}_{10}^{d2}$, $\tilde{\rho}_{10}^{d1}$, respectively, but

also by their complex conjugate terms. One part contains ρ_{00}^{21} , while the other ρ_{00}^{12} . As a result, when these diagonal elements are expressed via optical coherences, they acquire the sum $\rho_{00}^{21} + \rho_{00}^{12}$, which gives $\text{Re}(\rho_{00}^{21})$. This term reaches maximum value at the zero two-photon detuning and is responsible for the CPT effect. It is a known fact that for the Λ -scheme of levels the real part of the coherence is equal to 1/2 for $\delta = 0$ in the absence of the ground-state relaxation. Therefore $\rho_{00}^{22} + \rho_{00}^{11} - 2\text{Re}(\rho_{00}^{21}) \equiv 0$ (in the case of Λ -scheme of levels all populations are distributed between sublevels $m_{F_g} = 0$ and $\rho_{00}^{22} + \rho_{00}^{11} = 1$) and the excited state becomes unpopulated.

Considering the ground state, we account phenomenologically for the relaxation of its elements occurring due to collisions of alkali-metal atoms with particles of buffer gas and with the walls of an atomic cell. To do so, we introduce terms $-i\hbar\Gamma_g(\rho_{nn}^{mm} - 1/8)$ in equations for populations ρ_{nn}^{mm} . These terms describe the decay of the ground-state populations to the thermal equilibrium values 1/8. The relaxation of the coherence ρ_{00}^{21} is described by the same constant Γ_g , so the decay of the ground-state elements is isotropic. We consider the steady-state regime and therefore omit the time derivatives. Then the equations are as follows: Please remove if this is not the case.

$$\Gamma_g \rho_{-2-2}^{22} = -\Gamma \left[\frac{1}{3} \frac{V^2}{\Delta^2 + \Gamma^2} + \frac{V^2}{(\Delta + \omega_e)^2 + \Gamma^2} \right] \rho_{-2-2}^{22} + \frac{\Gamma_g}{8} + \gamma \left(\frac{1}{3} \rho_{-2-2}^{uu} + \frac{1}{6} \rho_{-1-1}^{uu} + \frac{1}{2} \rho_{-1-1}^{dd} \right), \quad (\text{A2a})$$

$$\Gamma_g \rho_{-1-1}^{22} = -\frac{1}{2} \Gamma \left[\frac{V^2}{\Delta^2 + \Gamma^2} + \Gamma \frac{V^2}{(\Delta + \omega_e)^2 + \Gamma^2} \right] \rho_{-1-1}^{22} + \frac{\Gamma_g}{8} + \gamma \left(\frac{1}{6} \rho_{-2-2}^{uu} + \frac{1}{12} \rho_{-1-1}^{uu} + \frac{1}{4} \rho_{00}^{uu} + \frac{1}{4} \rho_{-1-1}^{dd} + \frac{1}{4} \rho_{00}^{dd} \right), \quad (\text{A2b})$$

$$\Gamma_g \rho_{-1-1}^{11} = -\frac{1}{6} \Gamma \left[\frac{V^2}{\Delta^2 + \Gamma^2} + \Gamma \frac{V^2}{(\Delta + \omega_e)^2 + \Gamma^2} \right] \rho_{-1-1}^{11} + \frac{\Gamma_g}{8} + \gamma \left(\frac{1}{2} \rho_{-2-2}^{uu} + \frac{1}{4} \rho_{-1-1}^{uu} + \frac{1}{12} \rho_{00}^{uu} + \frac{1}{12} \rho_{-1-1}^{dd} + \frac{1}{12} \rho_{00}^{dd} \right), \quad (\text{A2c})$$

$$\begin{aligned} \Gamma_g \rho_{00}^{22} &= -\frac{1}{2} \Gamma \left[\frac{V^2}{\Delta^2 + \Gamma^2} + \frac{1}{3} \Gamma \frac{V^2}{(\Delta + \omega_e)^2 + \Gamma^2} \right] \rho_{00}^{22} + \frac{1}{2} \frac{V^2}{\Delta^2 + \Gamma^2} [\Delta \text{Im}(\rho_{00}^{21}) + \Gamma \text{Re}(\rho_{00}^{21})] \\ &\quad + \frac{1}{6} \frac{V^2}{(\Delta + \omega_e)^2 + \Gamma^2} [(\Delta + \omega_e) \text{Im}(\rho_{00}^{21}) + \Gamma \text{Re}(\rho_{00}^{21})] \\ &\quad + \frac{\Gamma_g}{8} + \gamma \left(\frac{1}{4} \rho_{-1-1}^{uu} + \frac{1}{4} \rho_{11}^{uu} + \frac{1}{12} \rho_{-1-1}^{dd} + \frac{1}{3} \rho_{00}^{dd} + \frac{1}{12} \rho_{11}^{dd} \right), \end{aligned} \quad (\text{A2d})$$

$$\begin{aligned} \Gamma_g \rho_{00}^{11} &= -\frac{1}{2} \Gamma \left[\frac{V^2}{\Delta^2 + \Gamma^2} + \frac{1}{3} \frac{V^2}{(\Delta + \omega_e)^2 + \Gamma^2} \right] \rho_{00}^{11} - \frac{1}{2} \frac{V^2}{\Delta^2 + \Gamma^2} [\Delta \text{Im}(\rho_{00}^{21}) - \Gamma \text{Re}(\rho_{00}^{21})] \\ &\quad - \frac{1}{6} \frac{V^2}{(\Delta + \omega_e)^2 + \Gamma^2} [(\Delta + \omega_e) \text{Im}(\rho_{00}^{21}) - \Gamma \text{Re}(\rho_{00}^{21})] \\ &\quad + \frac{\Gamma_g}{8} + \gamma \left(\frac{1}{4} \rho_{-1-1}^{uu} + \frac{1}{3} \rho_{00}^{uu} + \frac{1}{4} \rho_{11}^{uu} + \frac{1}{12} \rho_{-1-1}^{dd} + \frac{1}{12} \rho_{11}^{dd} \right), \end{aligned} \quad (\text{A2e})$$

$$\Gamma_g \rho_{11}^{22} = -\frac{1}{3} \Gamma \frac{V^2}{\Delta^2 + \Gamma^2} \rho_{11}^{22} + \frac{\Gamma_g}{8} + \gamma \left(\frac{1}{6} \rho_{22}^{uu} + \frac{1}{12} \rho_{11}^{uu} + \frac{1}{4} \rho_{00}^{uu} + \frac{1}{4} \rho_{11}^{dd} + \frac{1}{4} \rho_{00}^{dd} \right), \quad (\text{A2f})$$

$$\Gamma_g \rho_{11}^{11} = -\Gamma \frac{V^2}{\Delta^2 + \Gamma^2} \rho_{11}^{11} + \frac{\Gamma_g}{8} + \gamma \left(\frac{1}{2} \rho_{22}^{uu} + \frac{1}{4} \rho_{11}^{uu} + \frac{1}{12} \rho_{00}^{uu} + \frac{1}{12} \rho_{11}^{dd} + \frac{1}{12} \rho_{00}^{dd} \right), \quad (\text{A2g})$$

$$\Gamma_g \rho_{22}^{22} = \frac{\Gamma_g}{8} + \gamma \left(\frac{1}{3} \rho_{22}^{uu} + \frac{1}{6} \rho_{11}^{uu} + \frac{1}{2} \rho_{11}^{dd} \right), \quad (\text{A2h})$$

$$\begin{aligned} \left\{ \delta + i\Gamma_g + \frac{i}{2} \Gamma \left[\frac{V^2}{\Delta^2 + \Gamma^2} + \frac{1}{3} \frac{V^2}{(\Delta + \omega_e)^2 + \Gamma^2} \right] \right\} \rho_{00}^{21} &= \frac{i}{4} \Gamma \left[\frac{V^2}{\Delta^2 + \Gamma^2} + \frac{1}{3} \frac{V^2}{(\Delta + \omega_e)^2 + \Gamma^2} \right] (\rho_{00}^{22} + \rho_{00}^{11}) \\ &+ \frac{1}{4} \left[\Delta \frac{V^2}{\Delta^2 + \Gamma^2} + \frac{1}{3} (\Delta + \omega_e) \frac{V^2}{(\Delta + \omega_e)^2 + \Gamma^2} \right] (\rho_{00}^{22} - \rho_{00}^{11}). \end{aligned} \quad (\text{A2i})$$

The light shift of the ground-state microwave transition frequency is neglected in Eqs. (A2) to simplify calculations. To account for complete depolarization of the excited state, we replaced all its populations with the arithmetic mean: ρ_{ii}^{uu} , $\rho_{ii}^{dd} \rightarrow \left(\sum_{i=-2}^2 \rho_{ii}^{uu} + \sum_{i=-1}^1 \rho_{ii}^{dd} \right) / 8$. The solution for a significant rate of optical pumping, $V^2/\Gamma \gg \Gamma_g$, demonstrated that physical contrast, which we define here as $[\rho^{ee}(|\delta| \gg V^2/\Gamma) - \rho^{ee}(\delta = 0)] / \rho^{ee}(|\delta| \gg V^2/\Gamma)$, is twice greater when the excited state is depolarized. Here ρ^{ee} is the sum of populations of the excited-state sublevels.

Figure 1 demonstrates distributions of populations of ^{87}Rb $5\text{S}_{1/2}$ and $5\text{P}_{1/2}$ states for two cases: (a) without and (b) with excited-state depolarization. They were calculated for $\Gamma/2\pi = 1$ GHz, $\omega_e/2\pi = 817$ MHz, $\Delta/2\pi = -30$ MHz, $\delta = 0$. The value of the Rabi frequency was set to provide power broadening of the CPT resonance three times greater than Γ_g . In case (b) population of sublevel $m_{F_e} = 2$ decreases and optical pumping of the nonabsorbing sublevel $m_{F_g} = 2$ becomes smaller. Populations of excited-state sublevels $F_e = 2, m_{F_e} = -2, -1, 0, F_e = 1, m_{F_e} = -1, 0$ grow, which increases the amount of spontaneous transitions to working sublevels $F_g = 1, 2, m_{F_g} = 0$. We note that population of sublevel $F_g = 1, m_{F_g} = 1$ is smaller than that of $F_g = 1, m_{F_g} = -1$, since the probability of transition $|F_g = 1, m_{F_g} = 1\rangle \rightarrow |F_e = 2, m_{F_e} = 2\rangle$ is greater, while the repopulation rate of these sublevels is the same due to spontaneous transitions.

We note that Eq. (A2f) for coherence ρ_{00}^{21} contains terms proportional to $(\rho_{00}^{22} - \rho_{00}^{11})$ in its right-hand side. Despite bichromatic field components having equal intensities, populations of working sublevels are not equal due to spontaneous transitions. It is a known fact that in the case of unequal ground-state populations and nonzero optical detuning ($\Delta \neq 0$) the CPT resonance is asymmetric. This occurs since the real part of coherence ρ_{00}^{21} acquires a term proportional to δ [due to the presence of the

contribution proportional to $(\rho_{00}^{22} - \rho_{00}^{11})$ in Eq. (A2f)]. As a consequence, the CPT resonance becomes neither an even nor an odd function of δ . Also, in the case of asymmetry, equations for working sublevels $m_{F_g} = 0$ acquire terms that are proportional to optical detuning and difference $\rho_{00}^{21} - \rho_{00}^{12}$ [26]. We have replaced them in equations by the imaginary part for brevity.

Equations for ρ_{00}^{22} and ρ_{00}^{11} contain the real part of coherence due to the following considerations. In the case of the Λ -scheme of levels (only sublevels $F_g = 2, m_{F_g} = 0, F_g = 1, m_{F_g} = 0$, and $F_e = 2, m_{F_e} = 1$ are considered), the term, describing the transfer of atoms from the upper level to the ground-state populations due to spontaneous decay is $(1/4)(V^2/\Gamma)[1 - 2\text{Re}\rho_{00}^{21}]$ for $\Delta = 0$. In this situation, the real part of coherence is compensated by the term in the population of the excited state. See equation (A1f), where there is $\text{Re}(\rho_{00}^{21})$ with negative sign, while equations for populations of working sublevels have terms $\propto \text{Re}(\rho_{00}^{21})$ with positive sign. In our case, we have not expressed the excited-state populations in Eqs. (A2) via the ground-state elements to avoid equations being too bulky. However, even if we do so, there will not be a full compensation of the real part of coherence as in the case of the Λ -scheme of levels. This occurs since in our case there is a branching for spontaneous decay: populations ρ_{11}^{uu} and ρ_{11}^{dd} are transferred not only to working sublevels $m_{F_g} = 0$, but also to $\rho_{11}^{22}, \rho_{11}^{11}, \rho_{22}^{22}$. Therefore, the situation is more complex than in the case of Λ -scheme of levels and equations become more complicated.

In the case of complete depolarization of the excited state its populations are equal. As a result, spontaneous transitions equally populate working sublevels, providing a symmetric CPT resonance. Pay attention here to terms in equations for ground-state populations that are proportional to the spontaneous decay rate γ . The sum of coefficients standing before populations of the excited state is equal to 1 in each case. Therefore, when the condition

$\rho_{ii}^{uu} = \rho_{jj}^{uu} = \rho_{ii}^{dd} = \rho_{jj}^{dd}$ is fulfilled, an equal amount of atoms is transferred to the ground-state sublevels due to spontaneous decay of the excited state.

-
- [1] E. Arimondo, in *Progress in Optics*, Progress in Optics, Vol. 35, edited by E. Wolf (Elsevier, 1996), p. 257.
 - [2] R. Michalzik, in *VCSELs* (Springer, 2013), p. 19.
 - [3] S. Knappe, P. Schwindt, V. Gerginov, V. Shah, A. Branstrom, B. Lindseth, L.-A. Liew, H. Robinson, J. Moreland, Z. Popovic, L. Hollberg, and J. Kitching, in *14th International School on Quantum Electronics: Laser Physics and Applications*, Vol. 6604, edited by P. A. Atanasov, T. N. Dreischuh, S. V. Gateva, and L. M. Kovachev: International Society for Optics and Photonics (SPIE, 2007), p. 27.
 - [4] Y. Zhang, W. Yang, S. Zhang, and J. Zhao, Rubidium chip-scale atomic clock with improved long-term stability through light intensity optimization and compensation for laser frequency detuning, *J. Opt. Soc. Am. B* **33**, 1756 (2016).
 - [5] R. Vicarini, M. Abdel Hafiz, V. Maurice, E. Passilly, N. Kroemer, L. Ribetto, V. Gaff, C. Gorecki, S. Galliou, and R. Boudot, Mitigation of temperature-induced light-shift effects in miniaturized atomic clocks, *IEEE Trans. Ultrason. Ferroelectr. Freq. Control* **66**, 1962 (2019).
 - [6] S. Yanagimachi, K. Harasaka, R. Suzuki, M. Suzuki, and S. Goka, Reducing frequency drift caused by light shift in coherent population trapping-based low-power atomic clocks, *Appl. Phys. Lett.* **116**, 104102 (2020).
 - [7] M. Gozzelino, S. Micalizio, C. E. Calosso, A. Godone, and F. Levi, Kr-based buffer gas for rb vapor-cell clocks, *IEEE Trans. Ultrason. Ferroelectr. Freq. Control* **68**, 1442 (2020).
 - [8] V. Shah and J. Kitching, Advances in coherent population trapping for atomic clocks, *Adv. At., Mol., Opt. Phys.* **59**, 21 (2010).
 - [9] J. Vanier and C. Audoin, *The Quantum Physics of Atomic Frequency Standards* (A. Hilger, Philadelphia, 1989).
 - [10] J. Vanier, R. Kunski, N. Cyr, J. Y. Savard, and M. Tétu, On hyperfine frequency shifts caused by buffer gases: Application to the optically pumped passive rubidium frequency standard, *J. Appl. Phys.* **53**, 5387 (1982).
 - [11] W. Franzen and A. Emslie, Atomic orientation by optical pumping, *Phys. Rev.* **108**, 1453 (1957).
 - [12] R. Zhitnikov, P. Kuleshov, A. Okunovich, and B. Sevest'yanov, Optical orientation of ^{85}Rb and ^{87}Rb atoms by light of the D_2 line and relaxation in the $^2\text{P}_{3/2}$ state due to collisions with inert-gas atoms, *Sov. Phys. JETP* **31**, 445 (1970).
 - [13] A. Okunovich and V. Perel, Relaxation in the sublevel system of the excited state of alkali metal atoms colliding

with noble gas atoms, *Sov. J. Exp. Theor. Phys.* **31**, 356 (1970).

- [14] W. Happer, Optical pumping, *Rev. Mod. Phys.* **44**, 169 (1972).
- [15] J. Kitching, Chip-scale atomic devices, *Appl. Phys. Rev.* **5**, 031302 (2018).
- [16] F. A. Franz, R. Boggy, and C. E. Sooriemoorthi, Relative transition probabilities in deexcitation of atomic states by collisional quenching: $\text{Cs } 6^2p_{\frac{1}{2}} \rightarrow 6^2s_{\frac{1}{2}}$, *Phys. Rev. A* **11**, 1 (1975).
- [17] A. Sieradzan and F. A. Franz, Quenching, depolarization, and transfer of spin polarization in rb-n₂ collisions, *Phys. Rev. A* **25**, 2985 (1982).
- [18] G. A. Pitz, A. J. Sandoval, T. B. Tafoya, W. L. Klemmert, and D. A. Hostutler, Pressure broadening and shift of the rubidium D_1 transition and potassium D_2 transitions by various gases with comparison to other alkali rates, *J. Quant. Spectrosc. Rad. Trans.* **140**, 18 (2014).
- [19] A. Godone, F. Levi, S. Micalizio, and J. Vanier, Dark-line in optically-thick vapors: Inversion phenomena and line width narrowing, *Eur. Phys. J. D-At., Mol., Opt. Plasma Phys.* **18**, 5 (2002).
- [20] D. Adam Steck, Rubidium 87 d line data, <https://steck.us/alkalidata/>, 29 (2003).
- [21] D. Walter, W. Griffith, and W. Happer, Magnetic Slowing Down of Spin Relaxation Due to Binary Collisions of Alkali-Metal Atoms with Buffer-Gas Atoms, *Phys. Rev. Lett.* **88**, 093004 (2002).
- [22] S. Knappe, J. Kitching, L. Hollberg, and R. Wynands, Temperature dependence of coherent population trapping resonances, *Appl. Phys. B* **74**, 217 (2002).
- [23] C. T. R. Ardit M., Hyperfine relaxation of optically pumped rb 87 atoms in buffer gases, *Phys. Rev.* **136**, A643 (1964).
- [24] e. a. Pouliot A., Accurate determination of an alkali-vapor-inert-gas diffusion coefficient using coherent transient emission from a density grating, *Phys. Rev. A* **103**, 023112 (2021).
- [25] M. I. Vaskovskaya, E. A. Tsygankov, D. S. Chuchelov, S. A. Zibrov, V. V. Vassiliev, and V. L. Velichansky, Effect of the buffer gases on the light shift suppression possibility, *Opt. Express* **27**, 35856 (2019).
- [26] E. A. Tsygankov, S. V. Petropavlovsky, M. I. Vaskovskaya, D. S. Chuchelov, S. A. Zibrov, V. V. Vassiliev, V. L. Velichansky, and V. P. Yakovlev, Intensity nonlinearity of the error-signal frequency shift in the modulation spectroscopy of dark resonances and approaches to its reduction (2020).
- [27] V. Shah, V. Gerginov, P. D. D. Schwindt, S. Knappe, L. Hollberg, and J. Kitching, Continuous light-shift correction in modulated coherent population trapping clocks, *Appl. Phys. Lett.* **89**, 151124 (2006).